Statistical Analysis of a Mobile-to-Mobile Rician Fading Channel Model

Li-Chun Wang, *Senior Member, IEEE*, Wei-Cheng Liu, *Student Member, IEEE*, and Yun-Huai Cheng

Abstract—Mobile-to-mobile communication is an important application for intelligent transport systems and mobile ad hoc networks. In these systems, both the transmitter and receiver are in motion, subjecting the signals to Rician fading and different scattering effects. In this paper, we present a double-ring with a line-of-sight (LOS) component scattering model and a sum-of-sinusoids simulation method to characterize the mobile-to-mobile Rician fading channel. The developed model can facilitate the physical-layer simulation for mobile ad hoc communication systems. We also derive the autocorrelation function, level crossing rate (LCR), and average fade duration (AFD) of the mobile-to-mobile Rician fading channel and verify the accuracy by simulations.

Index Terms—Double-ring with a line-of-sight (LOS) component channel model, LOS component, mobile-to-mobile channel model, Rician fading, scattering, sum-of-sinusoids approximation method.

I. INTRODUCTION

MOBILITY significantly affects wireless networks. In traditional cellular systems, the base station is stationary, and only mobile terminals are in motion. However, in many new wireless systems, such as intelligent transport systems and mobile ad hoc networks, a mobile directly connects to another mobile without the help of fixed base stations. Thus, how mobility affects a system of which both the transmitter and receiver simultaneously move becomes an interesting problem.

From the propagation perspective, the scattering environment in the mobile-to-mobile communication channel is different from that in the base-to-mobile communication channel. In the former, both the transmitted and received signals are affected by the surrounding scatterers, whereas in the latter, only the mobile terminal is surrounded by many scatterers. It is the low height of the antenna that causes a ring of scatterers, and typically, high mobility units have a low antenna height. In a short-distance mobile-to-mobile communication link, it is likely that there exists a line-of-sight (LOS) or specular component between the transmitter and the receiver.

In the literature, most channel models for wireless communications were mainly developed for the conventional base-to-mobile cellular radio systems [2]–[5]. Whether these mobile-to-base channel models are applicable to the mobile-to-mobile communication systems remains unclear. Some, but not many, channel models had previously been studied. In [6], the theoretical performance of the mobile-to-mobile channel was developed. The authors in [7] introduced the discrete line spectrum method for modeling the mobile-to-mobile channel. However, the accuracy of this method was assured only for short-duration waveforms, as discussed in [8]. A simple but accurate sum-of-sinusoids method was proposed for modeling the mobile-to-mobile Rayleigh fading channel in [8]. The inverse fast Fourier transform (IFFT)-based mobile-to-mobile channel model was also proposed in [9]. Although it is the most accurate method compared with the discrete line spectrum and sum-of-sinusoids methods, the IFFT-based method requires a complex elliptic integration. In [10], the authors presented an analysis of measured radio channel statistics and their possible influence on the system performances in outdoor-to-indoor mobile-to-mobile communication channels. However, in [6]–[11], the effects of the LOS are all ignored.

To evaluate the performance of the physical layer, a simple channel simulator, such as Jakes' method in conventional cellular systems, is necessary. Related works on the mobile-to-mobile Rician fading channel include the following: In [12], a statistical model for a mobile-to-mobile Rician fading channel with Doppler shifts is presented. In [13], the model in [12] is employed to obtain the probability density function (pdf) of the received signal envelope, the time correlation function and radio frequency spectrum of the received signal, level crossing rates (LCRs), and average fade durations (AFDs).

This paper develops a sum-of-sinusoids mobile-to-mobile Rician fading simulator. First, the "double-ring with an LOS component" model is proposed to incorporate both the LOS and scattering effects. The double-ring scattering model was originally put forward [11], where the scatterers around the transmitter and the receiver were modeled by two independent rings. Second, the theoretical statistical property of the mobile-to-mobile Rayleigh channel is extended to the Rician fading case. The derived theoretical properties of the mobile-to-mobile Rician fading channel are employed to validate the accuracy of the proposed mobile-to-mobile Rician fading channel simulator involving a sum of sinusoids. Furthermore, the higher order statistics of the mobile-to-mobile Rician fading simulator, such as the LCR and AFD, is discussed. Compared with [12] and [13],

L.-C. Wang and W.-C. Liu are with the Department of Communication Engineering, National Chiao Tung University, Hsinchu 300, Taiwan (e-mail: lichun@cc.nctu.edu.tw; wcliu.cm92g@nctu.edu.tw).

Y.-H. Cheng was with the Department of Communication Engineering, National Chiao Tung University, Hsinchu 300, Taiwan. He is now with Mobinnova Corporation, Taoyuan 33059, Taiwan (e-mail: yunhuai.cheng@gmail.com).

this paper provides, in addition, the simulation and theoretical comparisons for the autocorrelation function of the fading envelope, the comparison between the fading envelope of double- and single-ring scattering models for different K factors, and the difference in the fading envelope of both the double- and single-ring scattering models for different K factors.

The rest of this paper is organized as follows: Section II describes the system model and the proposed "double-ring with an LOS component" scattering model. In Section III, the sum-of-sinusoids mobile-to-mobile Rician fading simulator is presented. Section IV analyzes the LCR and AFD. Section V shows the numerical results. In Section VI, concluding remarks are given.

II. SCATTERING ENVIRONMENT

This section describes a *double-ring with an LOS component scattering* model for the mobile-to-mobile Rician fading channel. For comparison purposes, the independent double-ring scattering model for the mobile-to-mobile Rayleigh fading channel is also presented.

A. Traditional Double-Ring Scattering Model

In a mobile-to-mobile communication channel, the antenna heights of both the transmitter and receiver are below the surrounding objects; it is thus likely that both the transmitter and receiver experience rich scattering effects in the propagation paths. Reference [11] showed an independent two-ring scattering environment for characterizing the mobile-to-mobile Rayleigh fading channel. According to this scattering model, a sum-of-sinusoids method was suggested to approximate the mobile-to-mobile Rayleigh fading channel. The scatterers are assumed to be uniformly distributed. Let the transmitter and receiver move at the speeds of $\mathbf{v}_1$ and $\mathbf{v}_2$, respectively. For all MN independent paths, the amplitude of the normalized complex signal received in the mobile-to-mobile Rayleigh fading channel can be expressed as

$$Y(t) = \sqrt{\frac{1}{MN}} \sum_{m=1}^{M} \sum_{n=1}^{N} \exp[j(2\pi f_1 t \cos \alpha_n + 2\pi f_2 t \cos \beta_m + \phi_{nm})] \quad (1)$$

where $f_1 = |\mathbf{v}_1|/\lambda$ and $f_2 = |\mathbf{v}_2|/\lambda$ are the maximum Doppler frequencies that result from the motion of transmission (TX) and reception (RX), respectively. $|\mathbf{v}|$ denotes the length of a vector $\mathbf{v}$, whereas λ is the carrier wavelength. In (1)

$$\alpha_n = \frac{2n\pi - \pi + \theta_n}{4N} \quad (2)$$

$$\beta_m = \frac{2(2m\pi - \pi + \psi_m)}{4M} \quad (3)$$

where the angles of departure in each scattering path θ_n and the angle of arrival ψ_m and ϕ_{nm} in $Y(t)$ are all independent uniform random variables over $[-\pi, \pi]$. It was proved in [4] and [11] that the autocorrelation function of the complex envelope $Y(t)$ is equal to

$$R_{YY}(\tau) = \frac{J_0(2\pi f_1 \tau) J_0(2\pi f_2 \tau)}{2} \quad (4)$$
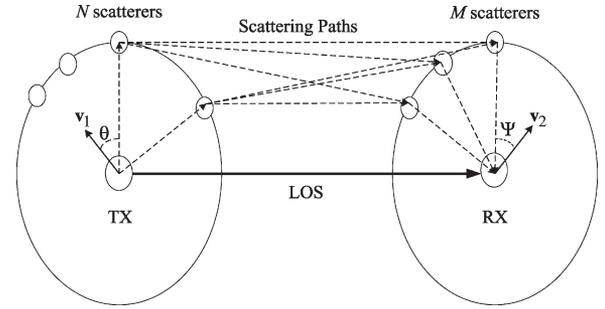

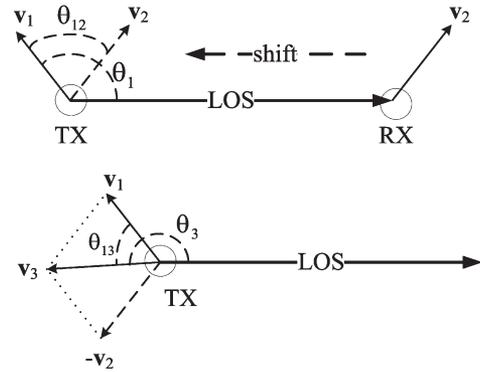Fig. 1. Scattering environment in a mobile-to-mobile system with an LOS component.

Fig. 2. Relative velocity $\mathbf{v}_3$ from the TX with velocity $\mathbf{v}_1$ to the RX with velocity $\mathbf{v}_2$.

where $J_0(\cdot)$ is the zeroth-order Bessel function of the first kind.

B. Double-Ring With an LOS Component Scattering Model

In some situations, certain LOS components exist between the transmitter and the receiver. Fig. 1 shows the proposed "double-ring with an LOS component" scattering model. In addition to the two scattering rings, an LOS component is added between the transmitter and the receiver. It is complex to present the LOS component by a mathematical formula, particularly when both the transmitter and receiver are in motion. Therefore, we use the concept of relative motion to simplify the problem. Fig. 2 shows the relative velocity $\mathbf{v}_3$ of the transmitter to the receiver if the velocity of the receiver is set to be zero. In the figure, θ_3 is the angle between $\mathbf{v}_3$ and the LOS component. The relative velocity of the transmitter $\mathbf{v}_3$ can be derived as follows:

$$|\mathbf{v}_3| = \sqrt{(|\mathbf{v}_1| \cos \theta_{12} - |\mathbf{v}_2|)^2 + (|\mathbf{v}_1| \sin \theta_{12})^2} \quad (5)$$

$$\theta_3 = \theta_1 + \theta_{13} \quad (6)$$

where θ_{12} is the angle between vectors $\mathbf{v}_1$ and $\mathbf{v}_2$, θ_1 is the angle between vector $\mathbf{v}_1$ and the LOS component, and the angle between vectors $\mathbf{v}_1$ and $\mathbf{v}_3$ is

$$\theta_{13} = \cos^{-1} \left(\frac{|\mathbf{v}_1|^2 + |\mathbf{v}_3|^2 - |\mathbf{v}_2|^2}{2|\mathbf{v}_1||\mathbf{v}_3|} \right). \quad (7)$$

Thus, the LOS component of the mobile-to-base station case can be expressed as

$$\text{LOS} = \sqrt{K} \exp\left[j(2\pi f_3 t \cos \theta_3 + \phi_0) \right] \quad (8)$$

where K is the ratio of the specular power to the scattering power, f_3 is the Doppler frequency caused by $\mathbf{v}_3$, and the initial phase ϕ_0 is uniformly distributed over $[-\pi, \pi)$.

III. SUM-OF-SINUSOIDS RICIAN FADING SIMULATOR

According to the "double-ring with an LOS component" scattering model shown in Fig. 1, a new sum-of-sinusoids Rician fading simulator for the mobile-to-mobile communication is developed.

A. Signal Model for Double-Ring With an LOS Component Scattering

Because Rayleigh fading is a special case of Rician fading without the specular component, the received complex signal of the mobile-to-mobile Rician fading channel is equivalent to the sum of the scattering signal and an LOS component. Therefore, with reference to (1) and (8), the received complex envelope of the mobile-to-mobile Rician fading channel can be written as

$$Z(t) = \frac{Y(t) + \sqrt{K} \exp\left[j(2\pi f_3 t \cos\theta_3 + \phi_0)\right]}{\sqrt{1+K}}. \qquad (9)$$

The complex signal $Z(t)$ is decomposed into the in-phase component $Z_c(t)$ and the quadrature component $Z_s(t)$. Then, it follows that

$$Z(t) = Z_c(t) + jZ_s(t) \qquad (10)$$

where

$$Z_c(t) = \frac{Y_c(t) + \sqrt{K} \cos(2\pi f_3 t \cos\theta_3 + \phi_0)}{\sqrt{1+K}} \qquad (11)$$

$$Z_s(t) = \frac{Y_s(t) + \sqrt{K} \sin(2\pi f_3 t \cos\theta_3 + \phi_0)}{\sqrt{1+K}} \qquad (12)$$

$$Y_c(t) = \Re\{Y(t)\} \qquad (13)$$

$$Y_s(t) = \Im\{Y(t)\}. \qquad (14)$$

B. Second-Order Statistics

The second-order statistical properties of $Z(t)$ are then derived. The autocorrelation function of $Z_c(t)$ can be calculated as

$$
\begin{aligned}
&R_{Z_c Z_c}(\tau) \\
&= \mathrm{E}\left[Z_c(t)Z_c(t+\tau)\right] \\
&= \frac{1}{1+K}\left\{ \frac{1}{MN}\mathrm{E}\left[\sum_{m=1}^{M}\sum_{n=1}^{N} \cos\left(2\pi(f_1\cos\alpha_n \right.\right.\right. \\
&\qquad\qquad\qquad\qquad\qquad\qquad + f_2\cos\beta_m)t + \phi_{nm}) \\
&\qquad\qquad\quad \times \sum_{p=1}^{N}\sum_{q=1}^{M} \cos\left(2\pi(f_1\cos\alpha_p + f_2\cos\beta_q) \right. \\
&\qquad\qquad\qquad\qquad\qquad\qquad\qquad \left.\left.\times (t+\tau)+\phi_{pq}\right)\right] \\
&\qquad + K\mathrm{E}\left[\cos(2\pi f_3 t\cos\theta_3 + \phi_0)\right. \\
&\qquad\qquad\qquad \left. \times \cos(2\pi f_3(t+\tau)\cos\theta_3 + \phi_0)\right] \\
&\qquad + \sqrt{\frac{K}{MN}}A + \sqrt{\frac{K}{MN}}B\right\}
\end{aligned} \qquad (15)
$$

where E is the statistical expectation operator

$$
\begin{aligned}
A = \mathrm{E}&\left[\sum_{m=1}^{M}\sum_{n=1}^{N} \cos\left(2\pi(f_1\cos\alpha_n + f_2\cos\beta_m)t + \phi_{nm}\right) \right. \\
&\left. \times \cos\left(2\pi f_3(t+\tau)\cos\theta_3 + \phi_0\right)\right] = 0
\end{aligned} \qquad (16)
$$

$$
\begin{aligned}
B = \mathrm{E}&\left[\cos(2\pi f_3 t\cos\theta_3 + \phi_0) \sum_{m=1}^{M}\sum_{n=1}^{N} \right. \\
&\left. \times \cos\left(2\pi(f_1\cos\alpha_n + f_2\cos\beta_m)(t+\tau) + \phi_{nm}\right)\right] = 0.
\end{aligned} \qquad (17)
$$

Because ϕ_{nm}, θ_n, ψ_m, and ϕ_0 are mutually independent random variables, $R_{Z_c Z_c}(\tau)$ can further be simplified as

$$
\begin{aligned}
&R_{Z_c Z_c}(\tau) \\
&= \frac{1}{1+K}\left\{ \frac{1}{2NM}\mathrm{E}\left[\sum_{n=1}^{N}\cos(2\pi f_1\tau\cos\alpha_n) \right.\right. \\
&\qquad\qquad\qquad\qquad \times \sum_{m=1}^{M}\cos(2\pi f_2\tau\cos\beta_m) \\
&\qquad\qquad\qquad\qquad - \sum_{n=1}^{N}\sin(2\pi f_1\tau\cos\alpha_n) \\
&\qquad\qquad\qquad\qquad\qquad \left.\times \sum_{m=1}^{M}\sin(2\pi f_2\tau\cos\beta_m)\right] \\
&\qquad + K\mathrm{E}\left[\cos(2\pi f_3 t\cos\theta_3 + \phi_0) \right. \\
&\qquad\qquad\qquad\qquad \left.\left.\times \cos(2\pi f_3(t+\tau)\cos\theta_3 + \phi_0)\right]\right\} \\
&= \frac{1}{1+K}\left[\frac{2}{\pi}\int_0^{\frac{\pi}{2}}\cos(2\pi f_1\tau\cos\alpha)\,d\alpha \right. \\
&\qquad\qquad\qquad \times \frac{1}{\pi}\int_0^{\pi}\cos(2\pi f_2\tau\cos\beta)\,d\beta \\
&\qquad\qquad\qquad - \frac{2}{\pi}\int_0^{\frac{\pi}{2}}\sin(2\pi f_1\tau\cos\alpha)\,d\alpha\frac{1}{\pi} \\
&\qquad\qquad\qquad\qquad \left. \times \int_0^{\pi}\sin(2\pi f_2\tau\cos\beta)\,d\beta\right] \\
&\qquad + \frac{K}{2(1+K)}\cos(2\pi f_3\tau\cos\theta_3).
\end{aligned} \qquad (18)
$$

Consequently

$$R_{Z_c Z_c}(\tau) = \frac{J_0(2\pi f_1\tau)J_0(2\pi f_2\tau) + K\cos(2\pi f_3\tau\cos\theta_3)}{2(1+K)} \qquad (19)$$
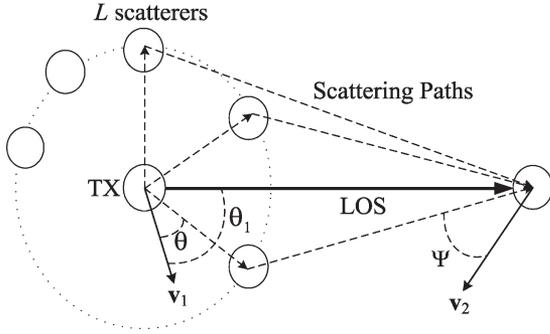
Fig. 3. Single-ring scattering environment for a mobile-to-mobile Rician fading channel.

is obtained. Similarly, other time correlation functions of $Z(t)$ can be obtained as follows:

$$R_{Z_s Z_s}(\tau) = \frac{J_0(2\pi f_1 \tau) J_0(2\pi f_2 \tau) + K \, \cos(2\pi f_3 \tau \, \cos \theta_3)}{2(1+K)} \tag{20}$$

$$R_{Z_c Z_s}(\tau) = \frac{K \, \sin(2\pi f_3 \tau \, \cos \theta_3)}{2(1+K)} \tag{21}$$

$$R_{Z_s Z_c}(\tau) = -\frac{K \, \sin(2\pi f_3 \tau \, \cos \theta_3)}{2(1+K)} \tag{22}$$

$$R_{ZZ}(\tau) = \frac{J_0(2\pi f_1 \tau) J_0(2\pi f_2 \tau) + K \, \exp(j 2\pi f_3 \tau \, \cos \theta_3)}{1+K}. \tag{23}$$

Similar derivation and results for mobile-to-base Rician fading channels can be found in [14]–[16].

C. Signal Model With Single-Ring Scattering

For comparison purposes, the Rician fading channel model developed from the single-ring scattering model is shown [6]. Note that the single-ring model developed for mobile-to-base channels may not be directly used for mobile-to-mobile channels. In Fig. 3, scatterers are distributed around the mobile terminal, and there exists an LOS component between the TX and the RX.

In this model, the received signal is the sum of signals from each scattering path with an LOS component. It was shown in [16] that the theoretical autocorrelation function of the complex envelope of the fading signal $Z(t)$ for the single-ring model is

$$R_{ZZ}(\tau) = \frac{J_0(2\pi f_1 \tau) + K \, \exp(j 2\pi f_3 \tau \, \cos \theta_3)}{1+K}. \tag{24}$$

We will see later in the numerical results that the new doubling-ring with an LOS component scattering model is more accurate than the single-ring model through the simulation.

IV. Higher Order Statistics

A. LCR

The fading envelope is denoted as $a(t)$, the derivative of the fading envelope as $\dot{a}(t)$, the pdf of the fading envelope as $p_a(a)$,

and the pdf of the slope of the fading envelope as $p_{\dot{a}}(\dot{a})$. Then, the LCR L_R of the fading envelope $|Z(t)|$ with respect to a specified level R can be calculated by [17]

$$L_R = \int_0^\infty \dot{a} p_{a,\dot{a}}(R, \dot{a}) \, d\dot{a} \tag{25}$$

where $p_{a,\dot{a}}(a, \dot{a})$ is the joint distribution function of a and $\dot{a}$. Now, the key issue is to find the joint distribution $p_{a,\dot{a}}(a, \dot{a})$.

From [18] and [19], we know that the joint distribution of the fading envelope and envelope slope of a Rician fading signal can be expressed as [20]

$$p_{a,\dot{a}}(a, \dot{a}) = \sqrt{\frac{1}{2\pi b_2}} \exp\left(-\frac{\dot{a}^2}{2b_2}\right)$$
$$\cdot \frac{a}{b_0} \exp\left(-\frac{a^2 + s^2}{2b_0}\right) I_0\left(\frac{as}{b_0}\right) \tag{26}$$

where

$$s^2 = \mathrm{E}\left[Z_c(t)\right]^2 + \mathrm{E}\left[Z_s(t)\right]^2$$
$$\Omega_p = \mathrm{E}[a^2] = s^2 + 2b_0$$
$$s^2 = \frac{K\Omega_p}{K+1}$$
$$2b_0 = \frac{\Omega_p}{K+1} \tag{27}$$

where $I_n(\cdot)$ is the modified nth-order Bessel function of the first kind. Ω_p is the square mean of the fading envelope, s^2 is the power of the specular component, and $2b_0$ is the scattered power. Note that (26) only holds when the frequency of the specular component f_s equals the carrier frequency f_c. This means that the Doppler shift of the specular component is zero. This situation only occurs when the impinging angle θ_3 is fixed at $90°$ or $270°$.

From (26), it is implied that a and $\dot{a}$ are mutually independent. Thus, we have

$$p_{\dot{a}}(\dot{a}) = \sqrt{\frac{1}{2\pi b_2}} \exp\left(-\frac{\dot{a}^2}{2b_2}\right) \tag{28}$$

$$p_a(a) = \frac{a}{b_0} \exp\left(-\frac{a^2 + s^2}{2b_0}\right) I_0\left(\frac{as}{b_0}\right). \tag{29}$$

Then, L_R can be simplified as

$$L_R = p_a(R) \int_0^\infty \dot{a} p_{\dot{a}}(\dot{a}) \, d\dot{a}$$
$$= p_a(R) \sqrt{\frac{b_2}{2\pi}} \tag{30}$$

where $b_2 = -d^2 R_{ZZ}(\tau)/d\tau^2|_{\tau=0}$ [19]. Recall that the autocorrelation function $R_{ZZ}(\tau)$ of the faded signal $Z(t)$ is derived in

(23). After derivation, b_2 can be expressed as

$$b_2 = \frac{2\pi^2 \left(f_1^2 + f_2^2 + 2K \cos^2 \theta_3 f_3^2 \right)}{K+1}. \tag{31}$$

Note that b_2 here is different from that in [16], which is $b_2 = 2\pi^2 b_0 f_3^2 (1 + 2 \cos^2 \theta_3)$. Because we consider the mobile-to-mobile double-ring model here, b_2 is a function of f_1, f_2, and f_3, but b_2 in [16] only associates with a single Doppler frequency f_3.

When θ_3 is $90°$ or $270°$, substituting (27) and (31) into (30) yields

$$L_R = \frac{2(K+1)R}{\Omega_p} \sqrt{\frac{b_2}{2\pi}} \exp\left(-K - \frac{(K+1)R^2}{\Omega_p} \right)$$
$$\cdot I_0 \left(2R\sqrt{\frac{K(K+1)}{\Omega_p}} \right). \tag{32}$$

For the general case where θ_3 can take a random value, the LCR has no closed-form solution. In [16], the LCR with uniform impinging angles was shown for the mobile-to-base Rician channels. For the special case of the single-ring model (i.e., $f_1 = f_3$ and $f_2 = 0$) with θ_3 being $90°$ or $270°$, b_2 can be simplified as that in [16], and (32) can be simplified to [16, eq. (16)].

From [16, eq. (15a)] with an assumption that θ_3 is uniformly distributed on $[0, 2\pi)$, we can also have

$$L_R = \sqrt{\frac{2(1+K)}{\pi \Omega_p}} R f_3 \cdot \exp\left[-K - \frac{(1+K)R^2}{\Omega_p} \right]$$
$$\cdot \int_0^\pi \left[1 + \frac{2}{R}\sqrt{\frac{\Omega_p K}{1+K}} \cos^2 \theta_3 \cdot \cos \alpha \right]$$
$$\cdot \exp\left[2R\sqrt{\frac{K(1+K)}{\Omega_p}} \cos \alpha - 2K \cos^2 \theta_3 \cdot \sin \alpha \right] d\alpha. \tag{33}$$

When θ_3 is $90°$ or $270°$, (33) can be simplified to (32).

B. AFD

According to the definition in [17], the AFD $\bar{\tau}_R$ for a specified level R is

$$\bar{\tau}_R = \frac{P(a \le R)}{L_R}. \tag{34}$$

Since the envelope of the signal is Rician distributed, $\bar{\tau}_R$ can be expressed as

$$\bar{\tau}_R = \frac{1 - Q\left(\sqrt{2K}, \sqrt{\frac{2(K+1)}{\Omega_p}} R \right)}{L_R} \tag{35}$$
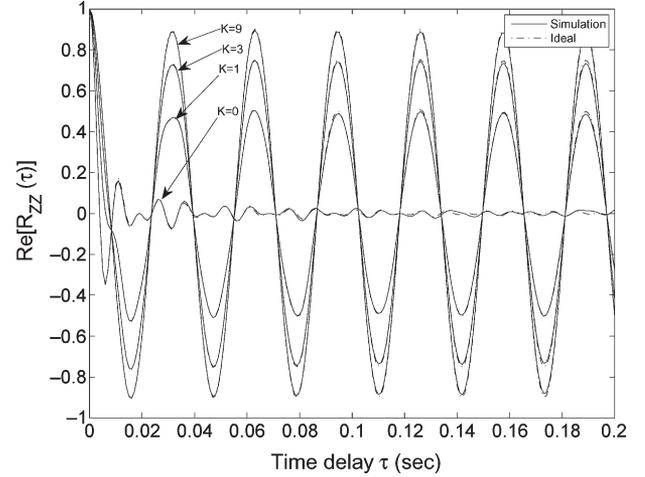

Fig. 4. Real part of the autocorrelation of the complex envelope $Z(t)$, where $N = M = 8$ for $K = 0, 1, 3,$ and 9.

where the Marcum's Q-function is defined as

$$Q(a,b) = \int_b^\infty x \exp\left(-\frac{x^2 + a^2}{2} \right) I_0(ax) \, dx. \tag{36}$$

V. NUMERICAL RESULTS

This section first validates the proposed sum-of-sinusoids mobile-to-mobile Rician fading simulator and then compares the correlation functions, pdf, and LCR and AFD of the proposed model with the theoretical values. Consider that the maximum Doppler frequencies for TX and RX are 100 and 20 Hz, respectively, and $\theta_1 = \pi/3$, $\theta_{12} = \pi/5$. From these values, we can find that $\theta_3 = 1.1865$.

A. Effects of the Rician Factor

Fig. 4 shows the correlation properties of the proposed sum-of-sinusoids mobile-to-mobile simulator. The solid line in the figure represents the theoretical value, whereas the dashed line represents the simulation results of the proposed channel model. Clearly, the two values match quite well for different Rician factors. Furthermore, for the same delay time τ, the magnitude of the channel correlation $R_{ZZ}(\tau)$ is proportional to the magnitude of the Rician factor K. With reference to (23), it can be seen that for a large enough delay time τ, $J_0(2\pi f_1 \tau) J_0(2\pi f_2 \tau) \approx 0$ and $J_0(2\pi f_1 \tau) J_0(2\pi f_2 \tau) \ll K \exp(2\pi f_3 \tau \cos \theta_3)$. Thus, it follows that

$$\Re\left\{ R_{ZZ}(\tau) \right\} \simeq \Re\left\{ \frac{K}{1+K} \exp(j2\pi f_3 \tau \cos \theta_3) \right\}$$
$$= \frac{K}{1+K} \cos(2\pi f_3 \tau \cos \theta_3). \tag{37}$$

Therefore, the maximum amplitude of the autocorrelation function $R_{ZZ}(\tau)$ is proportional to $(K/1+K)$ because $-1 \le \cos(2\pi f_3 \tau \cos \theta_3) \le 1$. As K increases, the peaks of $R_{ZZ}(\tau)$ are close to 1.
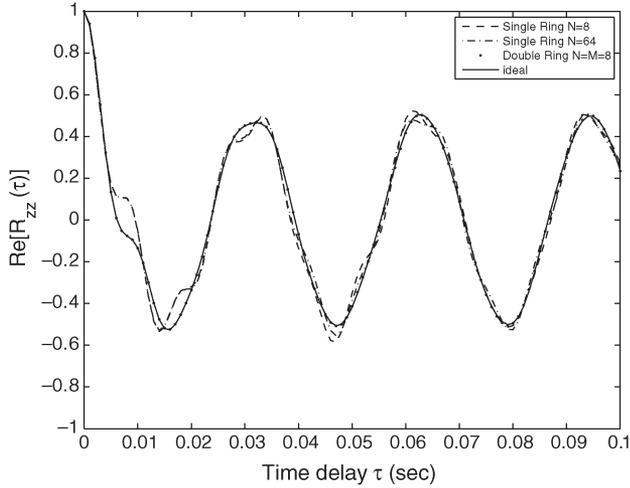
Fig. 5. Real part of the autocorrelation of the fading envelope of double- and single-ring scattering models for $K = 1$.

B. Comparison of a Double-Ring With an LOS Component Model and a Single-Ring Model

This part compares the proposed mobile-to-mobile Rician channel model developed from the double-ring with an LOS component scattering model with that developed from the single-ring scattering model [14] for different Rician factors and different numbers of scatterers. The main purpose of the comparison is to demonstrate that it is more suitable to employ the double-ring scattering model to characterize the mobile-to-mobile communication channel, i.e., the single-ring model developed for mobile-to-base channels may not be directly used for mobile-to-mobile channels. Fig. 5 show the correlation of the double-ring model with eight scatterers, the single-ring model with eight scatterers, the single-ring model with 64 scatterers, and the theoretical correlation functions for $K = 1$. Obviously, the double-ring model perfectly matches the ideal curve for $\Re[R_{ZZ}(\tau)]$ and yields better performance than the single-ring model, even when 64 scatterers are used in the single-ring model. The difference between the two scattering models is significant.

C. LCR and AFD

Fig. 6 shows the LCR of a mobile-to-mobile Rician channel fading envelope obtained using the sum-of-sinusoids method and that from theoretical analysis. As can be seen, the LCR decreases with the increase in the Rician factor. This phenomenon can be explained by the fact that channel fading has a greater correlation with a larger amount of LOS components. Once the correlation arises, the change in channel fading decreases.

Fig. 7 shows the analytical and simulated values of the normalized AFD for different Rician factors. As shown in the figure, the larger the Rician factor, the larger the AFD. This property is caused by the higher correlation of the fading envelope for a larger Rician factor. Thus, if the signal envelope fades below a specified level, it is less likely that it will exceed the level.

The numerical results for the LCR and AFD show some deviation of the simulation from the theoretical values, particularly
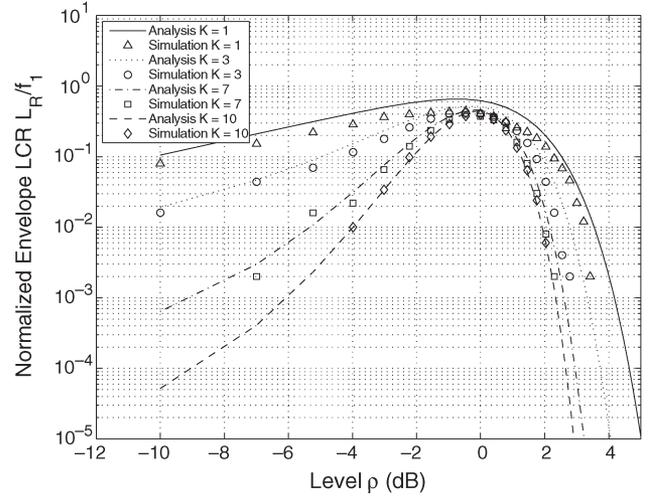

Fig. 6. Normalized envelope LCR for mobile-to-mobile Rician fading. The solid line denotes the theoretical results, whereas the dashed line denotes the simulation results, where $\rho = R/\sqrt{\Omega_p}$.
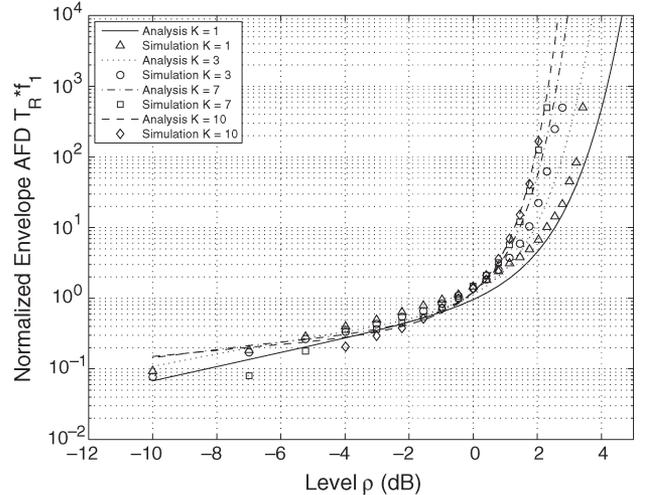

Fig. 7. Normalized AFD for a mobile-to-mobile Rician fading channel for $K = 1, 3, 7,$ and 10.

for small K (1 and 3). The simulation curves consistently fall below the analytical curves, which do not occur for the larger values of K. This is because when K is small, the scatterers will dominate the double-ring model. The simulation can only produce finite scatterers, which cannot approach the ideal case enough; thus, the deviation occurs. When K is large, the LOS term dominates the double-ring model; hence, the problem of finite number of scatterers is not very significant compared with the cases of small values of K.

VI. CONCLUSION

In this paper, a sum-of-sinusoids-based mobile-to-mobile Rician fading simulator has been developed. The double-ring scattering model was proposed to characterize the mobile-to-mobile communication environment with LOS components. Furthermore, the theoretical correlation functions of the mobile-to-mobile Rician channel were derived, and its accuracy was verified by simulations. The LCR and AFD of the

mobile-to-mobile Rician fading channel were derived. Finally, it was proved that the proposed sum-of-sinusoids approximation developed from the double-ring with an LOS component model can approach the theoretical value more closely than the single-ring model at a slightly higher cost of computational loads.

REFERENCES

[1] L.-C. Wang and Y.-H. Cheng, "A statistical mobile-to-mobile Rician fading channel model," in *Proc. IEEE Veh. Technol. Conf.*, Stockholm, Sweden, May 30–Jun. 1, 2005, vol. 1, pp. 63–67.

[2] P. Dent, G. E. Bottomley, and T. Croft, "Jakes fading model revisited," *Electron. Lett.*, vol. 29, no. 13, pp. 1162–1163, Jun. 1993.

[3] W. C. Jakes, *Microwave Mobile Communications*. Piscataway, NJ: IEEE Press, 1994.

[4] M. F. Pop and N. C. Beaulieu, "Limitations of sum-of-sinusoids fading channel simulator," *IEEE Trans. Commun.*, vol. 49, no. 4, pp. 699–708, Apr. 2001.

[5] C. Xiao, Y. R. Zheng, and N. C. Beaulieu, "Second-order statistical properties of the WSS Jakes' fading channel simulator," *IEEE Trans. Commun.*, vol. 50, no. 6, pp. 888–891, Jun. 2002.

[6] A. S. Akki and F. Haber, "A statistical model of mobile-to-mobile land communication channel," *IEEE Trans. Veh. Technol.*, vol. VT-35, no. 1, pp. 2–7, Feb. 1986.

[7] R. Wang and D. Cox, "Channel modeling for ad hoc mobile wireless networks," in *Proc. IEEE Veh. Technol. Conf.*, May 6–9, 2002, vol. 1, pp. 21–25.

[8] C. S. Patel, G. L. Stüber, and T. G. Pratt, "Simulation of Rayleigh-faded mobile-to-mobile communication channels," *IEEE Trans. Commun.*, vol. 53, no. 10, pp. 1876–1884, Oct. 2005.

[9] D. J. Young and N. C. Beaulieu, "The generation of correlated Rayleigh random variates by inverse discrete Fourier transform," *IEEE Trans. Commun.*, vol. 48, no. 7, pp. 1114–1127, Jul. 2000.

[10] I. Z. Kovács, P. C. F. Eggers, K. Olesen, and L. G. Petersen, "Investigations of outdoor-to-indoor mobile-to-mobile radio communication channels," in *Proc. IEEE Veh. Technol. Conf.*, Sep. 24–28, 2002, pp. 430–434.

[11] C. S. Patel, G. L. Stüber, and T. G. Pratt, "Simulation of Rayleigh faded mobile-to-mobile communication channels," in *Proc. IEEE Veh. Technol. Conf.*, Oct. 6–9, 2003, vol. 1, pp. 163–167.

[12] T. Tank and J.-P. M. G. Linnartz, "Statistical characterization of Rician multipath effects in a mobile-to-mobile communication channel," *Int. J. Wireless Inf. Netw.*, vol. 2, no. 1, pp. 17–26, Jan. 1995.

[13] J.-P. M. Linnartz and R. F. Diesta, "Evaluation of radio links and networks," in "PATH Research Program," Univ. California, Berkeley, CA, Tech. Rep. UCB-ITS-PRR-96-16, 1996.

[14] C. Xiao and Y. R. Zheng, "A statistical simulation model for mobile radio fading channels," in *Proc. IEEE Wireless Commun. Netw. Conf.*, Mar. 16–20, 2003, vol. 1, pp. 144–149.

[15] C. Xiao, Y. R. Zheng, and N. C. Beaulieu, "Statistical simulation models for Rayleigh and Rician fading," in *Proc. IEEE Int. Conf. Commun.*, May 16–20, 2003, pp. 3524–3529.

[16] C. Xiao, Y. R. Zheng, and N. C. Beaulieu, "Novel sum-of-sinusoids simulation models for Rayleigh and Rician fading channels," *IEEE Trans. Wireless Commun.*, vol. 5, no. 12, pp. 3667–3679, Dec. 2006.

[17] A. Papoulis, *Probability, Random Variables, and Stochastic Process*, 3rd ed. New York: McGraw-Hill, 1991.

[18] S. O. Rice, "Statistical properties of sine wave plus random noise," *Bell Syst. Tech. J.*, vol. 27, no. 1, pp. 109–157, Jan. 1948.

[19] A. S. Akki, "Statistical properties of mobile-to-mobile land communication channels," *IEEE Trans. Veh. Technol.*, vol. 43, no. 4, pp. 826–831, Nov. 1994.

[20] G. L. Stüber, *Principles of Mobile Communication*, 2nd ed. Dordrecht, The Netherlands: Kluwer, 2001.

Li-Chun Wang (S'92–M'96–SM'06) received the B.S. degree from the National Chiao Tung University, Hsinchu, Taiwan, in 1986, the M.S. degree from the National Taiwan University, Taipei, Taiwan, in 1988, and the M.Sc. and Ph.D. degrees from Georgia Institute of Technology, Atlanta, in 1995 and 1996, respectively, all in electrical engineering.

In 1995, he was affiliated with Bell Northern Research of Northern Telecom, Inc., Richardson, TX. From 1996 to 2000, he was with AT&T Laboratories, where he was a Senior Technical Staff Member with the Wireless Communications Research Department. Since August 2000, he has been an Associate Professor with the Department of Communication Engineering, National Chiao Tung University. He has authored more than 40 journal and 100 international conference papers. He is the holder of three U.S. patents. His current research interests are in the areas of adaptive/cognitive radio networks and cross-layer optimization for cooperative MIMO systems.

Prof. Wang served as an Associate Editor of the IEEE TRANSACTIONS ON WIRELESS COMMUNICATIONS from 2001 to 2006 and as a Guest Editor of the Special Issue on "Mobile Computing and Networking" of the IEEE JOURNAL ON SELECTED AREAS IN COMMUNICATIONS in 2005 and on "Radio Resource Management and Protocol Engineering in Future IEEE Broadband Networks" of the *IEEE Wireless Communications Magazine* in 2006. He was the organizing Chair of the MIMO Symposium for the First International Wireless Communications Mobile Computing Conference (IWCMC 2006) and the Technical Program Committee (TPC) Vice Chair of the IEEE VTS Asia Pacific Wireless Communications Symposium in 2006 and 2007. He is the TPC Co-Chair of the 2010 IEEE Vehicular Technology Conference. He was a corecipient (with G. L. Stüber and C.-T. Lea) of the 1997 IEEE Jack Neubauer Best Paper Award from the IEEE Vehicular Technology Society.

Wei-Cheng Liu (S'04) received the B.S. and M.S. degrees in electrical engineering from the National Tsing Hua University, Hsinchu, Taiwan, in 1999 and 2001, respectively. He is currently working toward the Ph.D. degree with the Department of Communication Engineering, National Chiao Tung University, Hsinchu.

After receiving the M.S. degree, he served his military service in Cheng Gong Ling, Taichung, Taiwan. In 2002, he was a GSM Layer 1 Software Engineer with Compal Communications, Inc., Taipei, Taiwan. His current research interests are in the areas of MIMO Rician channels in mobile ad hoc networks, cross-layer rate and power adaptation for wireless LANs, performance analysis for UWB systems, space–time–frequency code design, and cooperative network coding.

Yun-Huai Cheng was born in Taiwan in 1981. He received the B.Sc. degree in electrical and control engineering and the M.Sc. degree from the National Chiao Tung University, Hsinchu, Taiwan, in 2003 and 2005, respectively.

He is currently with Mobinnova Corporation, Taoyuan, Taiwan. His research interests are in the field of wireless communications.